HOSTED BY

ELSEVIER

CrossMark

Available online at www.sciencedirect.com

ScienceDirect

Progress in Natural Science: Materials International 25 (2015) 159–168

Progress in Natural Science Materials International

www.elsevier.com/locate/pnsmi
www.sciencedirect.com

Original Research

Effect of equal channel angular pressing on aging treatment of Al-7075 alloy

M.H. Shaeri[a,*], M. Shaeri[b], M.T. Salehi[c], S.H. Seyyedein[c], M.R. Abutalebi[c]

[a]Department of Metallurgy and Materials Engineering, Engineering Faculty, Imam Khomeini International University, Qazvin 34149-16818, Iran
[b]Department of Materials Science and Engineering, Sharif University of Technology, Tehran 11365-9466, Iran
[c]Department of Metallurgy and Materials Engineering, Iran University of Science and Technology (IUST), Tehran 16846-13114, Iran

Received 11 September 2014; accepted 17 November 2014
Available online 6 May 2015

Abstract

The effect of aging treatment on microstructure and mechanical properties of equal channel angular pressed Al-7075 alloy was examined. Commercial Al-7075 alloy in the solid solution heat-treated condition was processed by equal channel angular pressing through route B_C at both the room temperature and 120 °C. Only three passes of equal channel angular pressing was possible due to the low ductility of the alloy at both temperatures. Followed by equal channel angular pressing, the specimens have been aged at 120 °C for different aging times. Mechanical properties were measured by Vickers microhardness and tensile tests and microstructural observations were undertaken using transmission electron microscopy, X-ray diffractometer as well as optical microscopy. Microstructural investigations showed that ultrafine-grained materials with grain size in the range of 200–350 nm and 300–500 nm could be obtained after three passes of equal channel angular pressing at room temperature and 120 °C, respectively. Equal channel angular pressing of solid solution heat-treated Al-7075 alloy accelerates precipitation rate and subsequently leads to a significant decrease in aging time to attain maximum mechanical properties. Furthermore, it is possible to achieve maximum mechanical properties during equal channel angular pressing at 120 °C as a result of dynamic aging and formation of small η′ phase.
© 2015 Chinese Materials Research Society. Production and hosting by Elsevier B.V. This is an open access article under the CC BY-NC-ND license (http://creativecommons.org/licenses/by-nc-nd/4.0/).

Keywords: Equal channel angular pressing; Grain refinement; Aging treatment; TEM; Mechanical properties

1. Introduction

Equal channel angular pressing (ECAP) or extrusion (ECAE) is the most well developed procedure among the potential severe plastic deformation (SPD) processing techniques for modifying microstructure and producing ultrafine-grained (UFG) bulk materials [1]. This procedure has the advantage of fabricating fully dense materials without the introduction of any contaminants and large enough for real structural applications. Since there is no change in the cross-sectional dimensions of the specimen during the process, it is now well recognized as a promising method to enhance the strength of various metallic alloys through the occurrence of grain refinement in severe plastic deformation [2,3]. The intense plastic strain can be achieved by simple shear by pressing the specimen through a die containing two channels, equal in cross section, intersecting at an angle of Φ and with a corner curvature angle, Ψ, [4,5]. Previous studies on ECAP demonstrate that the main experimental factors influence properties and microstructural characteristics of ECAPed billets are processing route (rotation of the billet between successive passes), number of passes (N), die angle (Φ), corner curvature angle (Ψ) and the temperature of the pressing operation [6–9].

High strength aluminum alloys, such as the Al 7075-T6 alloy, that possess high strength/density ratio and reasonable high fracture toughness, are extensively used in the aerospace industry and structural applications [10,11]. It is well known that heat-treatable aluminum-based alloys can be strengthened by using of solid solution and dispersion hardening [12]. An effective technique to improve the properties is to develop Al alloys with UFG microstructures by SPD process such as ECAP [13,14]. During ECAP process of age-hardenable Al alloys, significant grain refinement as well as dislocation hardening occur together with precipitation hardening [8,15,16]. Therefore, combination of these three processes (solution treatment, aging and

*Corresponding author. Tel.: +9828 33901190; fax: +9828 33780073.
E-mail address: shaeri@ENG.ikiu.ac.ir (M.H. Shaeri).
Peer review under responsibility of Chinese Materials Research Society.

http://dx.doi.org/10.1016/j.pnsc.2015.03.005
1002-0071/© 2015 Chinese Materials Research Society. Production and hosting by Elsevier B.V. This is an open access article under the CC BY-NC-ND license (http://creativecommons.org/licenses/by-nc-nd/4.0/).

ECAP) may help to attain superior properties due to the high dislocation density and very fine precipitate distributions in the UFG microstructure [17]. In practice the formation of precipitates in the solution treated age-hardenable Al alloys leads to decline the formability of the processed material. Hence, cracking or segmentation of the material is expected during ECAP process at ambient temperature [8,18,19].

The aim of this work is to investigate the post-ECAP aging of Al-7075 alloy processed by ECAP in the solid solution heat treated condition. For this purpose mechanical properties (microhardness and strength) and microstructure of processed materials at two temperatures (room temperature (RT) and 120 °C) have been studied at various aging times in order to obtain the optimum aging condition. The microstructure was analyzed by Transmission electron microscopy (TEM) and optical microscopy (OM) as well as an X-ray diffractometer (XRD).

2. Experimental procedure

The Al-7075 alloy was received as extruded rods having the composition shown in Table 1. Prior to ECAP, $7 \times 7 \times 50$ mm^3 rectangular billets were cut from the as-received rod (parallel to the extrusion direction of the rod). The billets were solution heat treated at 470 °C for 1 h and then water quenched to form a super saturated solid solution (SSS). All the specimens were processed by ECAP at RT and 120 °C up to 3 passes immediately after quenching. Further ECAP passes leads to the formation of catastrophic cracking and segmentation. ECAP was conducted through a die with a channel angle of 90° and a curvature angle of 20° using a pressing speed of 0.5 mm s^{-1} with MoS_2 as a lubricant. The image of applied die and employed coordinate system was presented in our previous papers [18,20]. In order to avoid crack formation during ECAP process, back-pressure of 180 MPa was applied within the outlet ECAP channel by plunger of hydraulic valve. All pressings were conducted by rotating each billet about the longitudinal axis by 90° in the same direction between consecutive passes (designated as route B_C). It has been shown experimentally that, route B_C appears preferable for obtaining equiaxed grains with high angle boundaries, while refining grains through ECAP [20,21]. Following ECAP, the specimens were aged at 120 °C for different periods of time. For high temperature ECAP, the ECAP die was preheated to 120 °C and maintained for 15 min before inserting a specimen into the entrance channel. All the specimens were held inside the ECAP die for 5 min before pressing.

Vickers microhardness and tensile test were conducted to evaluate the mechanical properties of ECAPed specimens. Prior to microhardness measurement the billets were sectioned perpendicular to their longitudinal axes and then polished to a mirror-like finish. Indentation and microhardness measurements were undertaken with a Mitutoyo HM-124 microhardness tester equipped with a Vickers indenter under a load of 1 Kg and 15 s dwell time in accordance with ASTM: E-384. All microhardness data were at least the average of 20 indentations. The tensile tests were performed at room temperature using an Instron type testing machine operating at a constant rate of crosshead speed of 1 mm/min. Tensile test specimens with cross-section of 2.0 mm × 1.5 mm and gauge length of 10 mm were wire cut From ECAP processed specimens parallel to the pressing direction according to ASTM: E-8M.

Table 1
The chemical composition of as-received Al 7075 alloy (in wt. %).

Al	Si	Fe	Cu	Mn	Mg	Cr	Zn	Ti
Base	0.07	0.09	1.50	0.04	2.65	0.21	5.70	0.02

Microstructural characterization of the specimens before and after ECAP was performed by optical microscopy as well as TEM using a JEOL JEM 3010 transmission electron microscope operating at accelerating voltage of 300 kV. The specimens for optical examination were prepared from the cross section of the extruded billets (perpendicular to the pressing direction (ED-plane)) using standard polishing techniques and then etched with Keller's etchant containing HF:HCl:HNO_3:H_2O in a proportion of 2:3:5:190. For TEM investigations, 0.5 mm thick discs were sectioned from the cross section of the extruded billets (ED-plane), and then mechanically ground down to about 15 μm thick foils. Subsequently 3 mm discs were punched from the specimens and finally polished to perforation using a twin-jet electro polishing facility with a solution of 30% nitric acid in methanol at −25 °C and 15 V. Selected area electron diffraction (SAED) patterns were taken from an area with diameter of 2 μm. XRD measurements were also performed by using a RIGAKU, D/MAX-2500 X-ray diffractometer with Cu Kα radiation in order to identify the alloy phases present after ECAP. XRD specimens were taken from cross section of the billets after the final ECAP pass.

3. Results

3.1. Mechanical properties

3.1.1. Microhardness

As described above, in order to obtain optimum post-aging time of ECAP processed specimens, Vickers microhardness of the specimens were measured after aging treatment at 120 °C for various aging times. Fig. 1 shows the effect of aging time on the microhardness of un-ECAPed specimen and specimens subjected to ECAP process for 1, 2 and 3 passes at room temperature and 120 °C. As can be seen in Fig. 1(a), 24 h aging treatment was required for attaining peak microhardness in un-ECAPed specimens, while peak microhardness was achieved after 15, 12 and 9 h aging treatment for the specimens ECAPed at RT for 1 pass, 2 and 3 passes, respectively. Therefore it can be concluded that by increasing pass number, the aging time for attaining peak microhardness decreases significantly. Furthermore, microhardness versus aging time curve of ECAP processed specimens at 120 °C (Fig. 1(b)) demonstrates that, peak microhardness is achieved after 9 h aging treatment of 1 pass and 2 passes ECAPed specimen and

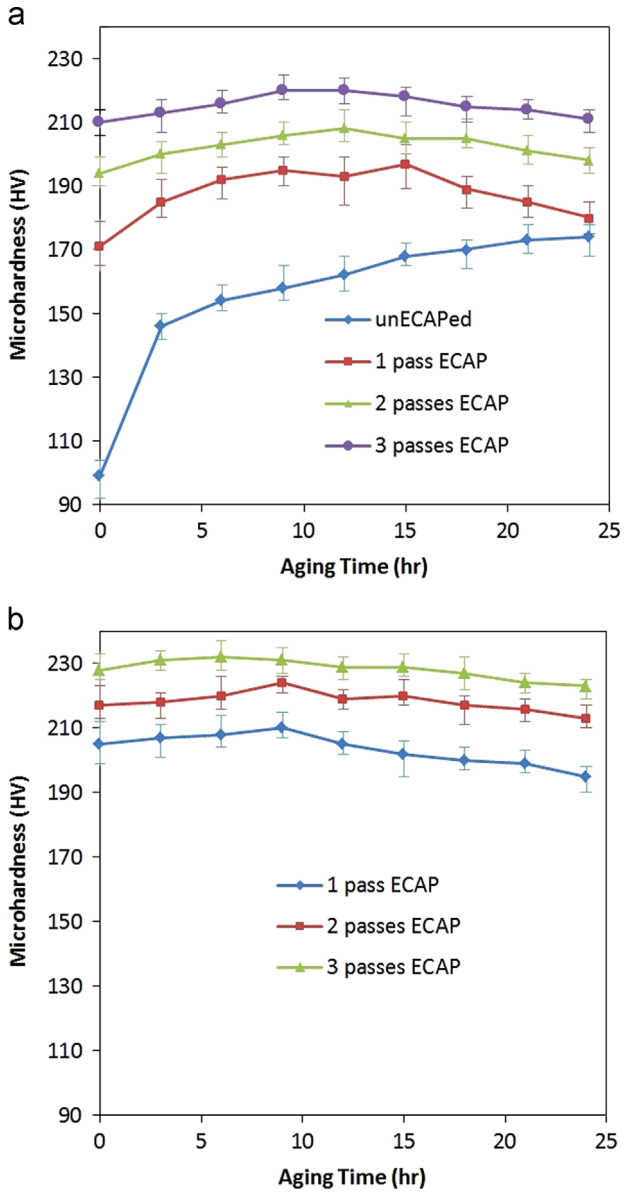

Fig. 1. Effect of aging time at 120 °C on microhardness of Al-7075 alloy subjected to ECAP process for 1, 2 and 3 passes at (a) room temperature and (b) 120 °C.

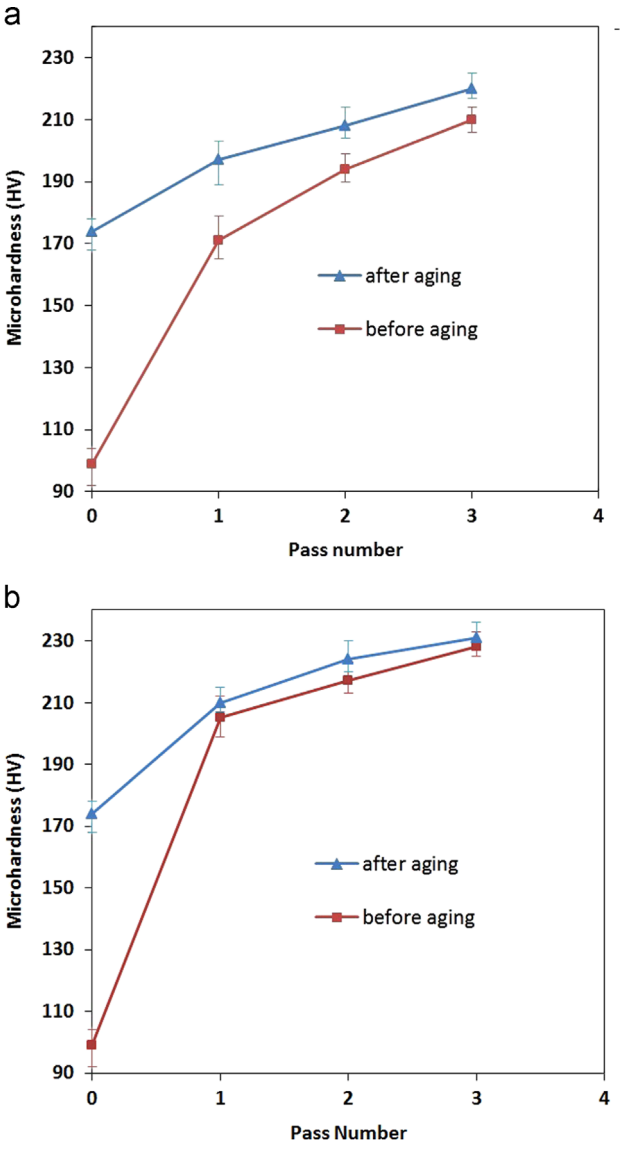

Fig. 2. Effect of pass number on microhardness of ECAP processed specimens before and after post-ECAP peak aging treatment, (a) ECAP processed at RT and (b) ECAP processed at 120 °C.

6 h aging treatment of 3 passes ECAPed specimen. It is apparent that ECAP process causes significant increment in peak aging time and also by increasing ECAP temperature the decline in peak aging time decreases.

The effect of pass number on the microhardness of ECAP processed specimens before and after post-ECAP peak aging (aging at 120 °C for attaining peak microhardness) is illustrated in Fig. 2. This figure shows that the microhardness of the solid solution specimen has increased significantly from 99 HV to 171 HV and 205 HV after one pass of ECAP at room temperature and 120 °C, respectively. As can be seen, increasing the pass number caused an increment in the microhardness of the specimens. Another important finding from Fig. 2 is that the effect of the first pass is more profound compared to the subsequent passes. Comparing the microhardness results of ECAP processed specimens at room temperature and 120 °C (Fig. 2(a)) and (Fig. 2(b)) reveal that the microhardness of the specimens processed at 120 °C is about 10–15% higher than that of the specimens processed at room temperature. On the other hand, the effect of post-ECAP aging treatment on the microhardness of processed specimens at 120 °C is negligible, while post-ECAP aging treatment leads to about 10% increment on the microhardness of ECAP processed specimens at RT. The reason of negligible effect of post-ECAP aging on the microhardness of ECAPed specimens at high temperature lies in dynamic strain aging during ECAP process.

3.1.2. Tensile behavior

Fig. 3 shows the engineering stress–strain curves of ECAP processed specimens at RT and 120 °C, post-ECAP peak age-hardened specimens and T6 specimen without any ECA pressing. The stress–strain curves show that yield strength

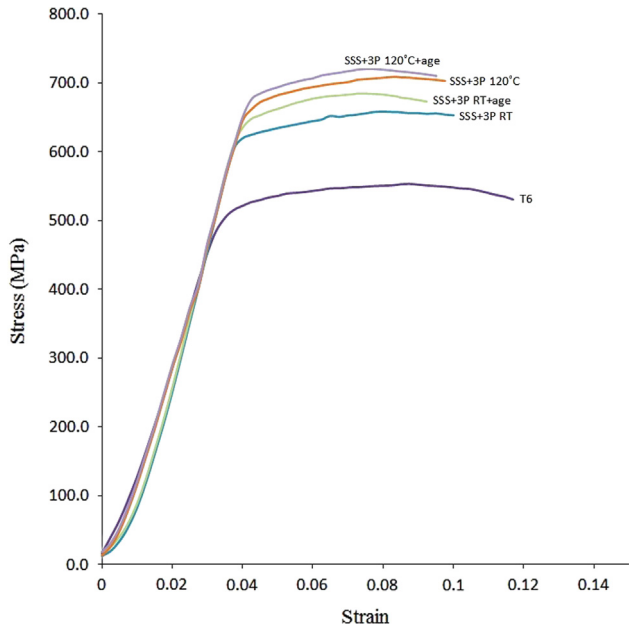

Fig. 3. Engineering stress–strain curves ofAl-7075 alloy at various ECAP and aging condition.

(YS) and ultimate tensile strength (UTS) of ECAPed specimen at 120 °C are higher than those of ECAPed specimen at RT, while elongation values of processed material at both RT and 120 °C are approximately the same. The YS and UTS of the post-ECAP peak age hardened specimen which ECAP processed at 120 °C are 685 and 720 MPa, respectively, which are about 34% and 30% higher, respectively, than those of the T6 Specimen (510 and 554 MPa). The elongation to failure of the post-ECAP peak age hardened specimen (9.5%) is smaller than that of the T6 specimen (11.7%). Another important result from these curves is that post-ECAP aging of pressed specimen at 120 °C has negligible effect on strength of the specimen, while post-ECAP aging of pressed specimen at RT leads to about 5% increase on strength of ECAPed specimen. It has been observed that the pressed specimens are both stronger and less ductile by comparison with the T6 specimen. These trends are consistent with data reported for other materials processed by ECAP [22–24]. In general, it is obvious that tensile test results are reasonably in good agreement with microhardness data.

3.2. Microstructure

3.2.1. Optical microscopy

Fig. 4(a) shows the appearance of the microstructure of starting material (unECAPed specimen) in the optical microscope after 24 h aging treatment at 120 °C (T6 condition). As can be seen in Fig. 4(a) the microstructure of starting material in T6 condition consists of large grains with a grain size in the range of 30 to 100 μm, and sub-grains with a grain size of less than 10 μm. The average grain size of the initial microstructure calculated by area fraction method is observed to be about 60 μm.

Fig. 4(b), (c) and (d) illustrate the OM micrographs of ECAP processed alloy for one, two and three passes at RT, respectively. As shown in Fig. 4(b), after 1 pass of ECAP the grain width decreases and deformation bands develop within the grains. Detailed inspection of the microstructural characteristics of 1 pass ECAPed specimen demonstrates that, the grains which were initially equiaxed, become considerably elongated along the TD direction equivalent to the horizontal direction at the point of exit from the ECAP die, and also within these grains, there is much evidence for shearing bands in a direction essentially perpendicular to the TD direction [25–29].

The microstructure observation of 2 passes ECAP processed specimen reveals that (Fig. 4(c)), some grains become more elongated and grain boundaries tend to lie approximately at 45° to the TD direction, and within the individual grains, there are shearing bands approximately parallel to the TD direction [25–29].

After 3 passes of ECA pressing the amount of deformation bands seems to increase and their distribution becomes more homogeneous, as shown in Fig. 4(d). It is apparent that the microstructure of 3 passes ECAPed specimen is very complex and the grain boundaries are not distinct on the specimen's surface. Deformation bands are visible within the grains but there appear to be no well-defined angular relationships. Generally, the OM results show that, the refining of the microstructure is observed with increasing the number of passes [25–29].

3.2.2. X-ray diffraction

XRD analysis was additionally performed to confirm the microstructural results obtained. Fig.5 displays the XRD results of unECAPed specimens in T6 and annealed conditions as well as ECAP processed specimens at RT and 120 °C before and after post-ECAP peak aging. The XRD data of annealed specimen (heated for 1 h at 415 °C followed by furnace cooling) was presented for determining the exact 2θ angle of η ($MgZn_2$) peaks. The indexes of diffraction planes of the hexagonal η ($MgZn_2$) were also indicated in the figure. As stated by Zhao et al. [30] and Cardoso et al. [27] the broad peak at about 20° are from the G-P zones, and the other weak peaks whose positions are a little lower than those of hexagonal η phase correspond to the metastable hexagonal η′ phase, whose lattice parameters are a little different from those of η phase. Comparing the intensity of the broad peaks at about 20° in Fig. 5 reveals that the volume fraction of G-P zones in ECAP processed specimen at RT is higher than that of the T6 specimen and ECAP processed specimen at 120 °C. As shown in Fig. 5 the G-P zones peak approximately disappears after post-ECAP aging of ECAP processed specimens at RT and 120 °C, so it can be concluded that the volume fraction of G-P zones significantly decreases after post-ECAP aging. Similarly, XRD patterns indicate that the volume fraction of η′ phase in post-ECAP age hardened specimens is larger than that of the other specimens, and also amount of η′ phase in ECAPed specimen at RT is very low. Therefore, it can be deduced from XRD results that the precipitates in ECAPed specimen at RT and post-ECAP age hardened specimens (both specimens ECAPed at RT and 120 °C) is mainly composed of G-P zones and η′ phase, respectively, while the precipitates in

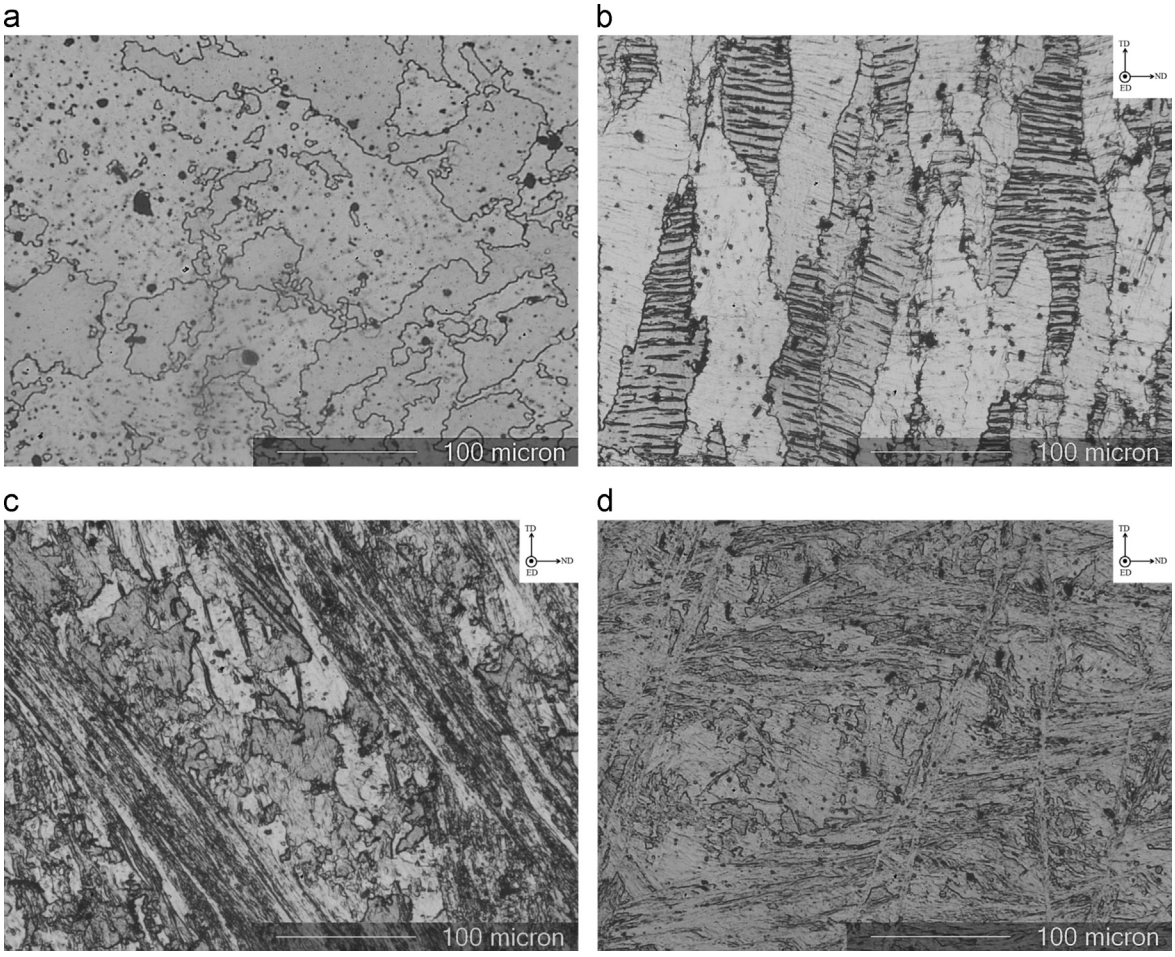

Fig. 4. Optical microstructures of Al-7075 alloy after ECAP at room temperature (cross section), (a) unECAPed, (b) 1 pass ECAPed, (c) 2 passes ECAPed and(d) 3 passes ECAPed.

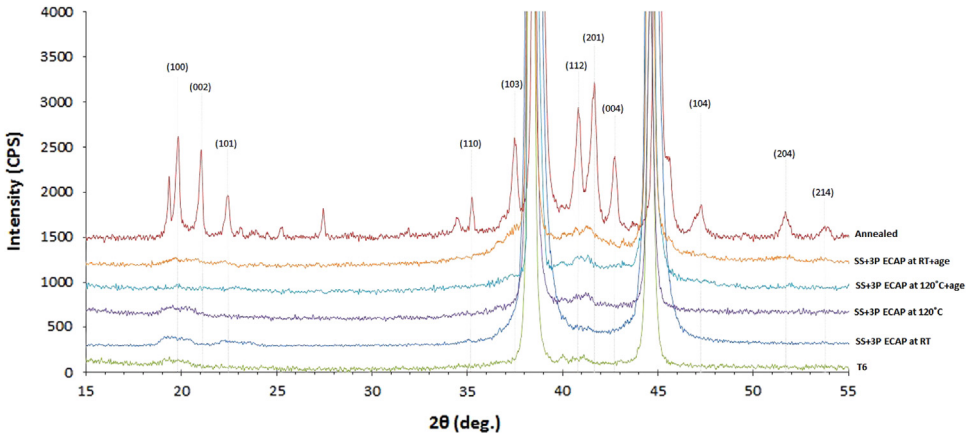

Fig. 5. XRD results of T6 specimen, ECAP processed specimen at RT and 120 °C before and after post-ECAP peak aging, and annealed specimen.

the T6 specimen and ECAPed specimen at 120 °C is composed of both G-P zones and η´ phase.

3.2.3. Electron microscopy

TEM images and corresponding SAED pattern of unECAPed Al-7075 alloy in T6 heat treatment condition are shown in Fig. 6. Careful inspection over a wide area showed that some subgrains of 2–5 μm in diameter can be observed in the microstructure of starting material. As described in the previous section (optical microscopy), the grain size is in the range of 30 to 100 μm, so it is not possible to show the grains distribution completely By TEM. Precipitates characterization of the T6 specimen reveals that two types of precipitates coexist, $MgZn_2$ plate-like precipitates with a size in range of

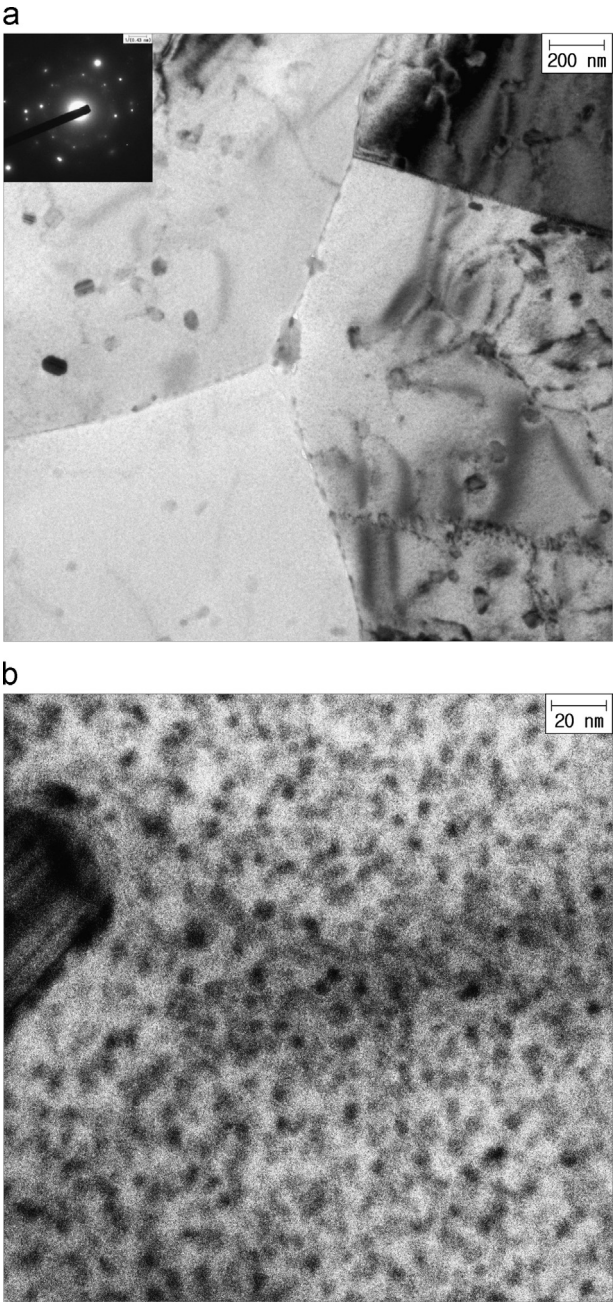

Fig. 6. TEM images and corresponding SAED patterns of the unECAPed Al-7075 alloy in T6 heat treatment condition.

40–80 nm (Fig. 6a) and η´ precipitates with a size in range of 5–10 nm (Fig. 6b). In fact, similar precipitates characterization presented by Park et al. [31,32] and Gjonnes et al. [33] which stated that most of the particles in the microstructure of 7075-T6 Al alloy are η´ transition phase and also minor quantities of G-P zones probably exist in T6 microstructure but their size is too small to be imaged. Thus, it can be seen from XRD results (Fig. 5) and TEM investigation (Fig. 6) that both G-P zones and η´ phase present in the microstructure of the T6 specimen.

Fig. 7 shows TEM micrograph of specimens subjected to three passes of ECAP process by route B_C at RT and 120 °C. As can be seen the grains of initial material with average grain size of about 60 μm refine to grains with average grain size less than 500 nm after three passes of ECAP. The microstructural comparison of the specimens (Fig. 7) demonstrates that the grain size of the specimen processed at RT is in the range of 200–350 nm, while the grain size of the specimen processed at 120 °C is in the range of 300–500 nm. So it can be concluded that the ECA pressing at RT is more effective for grain refinement. Bigger grain size of specimen processed at 120 °C compared with that of specimen processed at RT can be due to the fact that the higher processing temperature leads to lower stress on the samples and accordingly this produces larger final grain size [27]. As shown in Fig. 8 the amount of strain in shear bands and also the number of shear bands in ECAPed specimen at RT are considerably lower than those in ECAPed specimen at high temperature. The shear bands in ECAPed specimen at RT are sharp and exert high strain to specimen, while by increasing ECAP temperature the strain of shear bands decreases significantly and consequently the grain size increases. On the other hand, the increment in grain size by increasing ECAP temperature can be also related to the dynamic recovery and grain growth processes of the UFG microstructures occurring at elevated temperature.

It is also obvious from Fig. 7 that the grains after three passes are reasonably equiaxed and high density of dislocations is present especially at cell boundaries and the most of the grain boundaries are wavy and ill-defined. In specimen processed at 120 °C the dislocation density within the cells slightly diminished and more defined cell boundaries were formed, as compared to specimen processed at RT [27,30,34,35]. The corresponding SAED patterns are shown at the bottom of each TEM micrograph in Fig. 7. It is apparent that, the SAED patterns consist of rings of diffraction spots showing most of the grain boundaries have high angles of misorientation, while, sharper and more continuous rings in SAED pattern of processed specimen at RT compared with those of processed specimens at 120 °C demonstrate that the volume fraction of high angle grain boundaries (HABs) decreases by increasing processing temperature of Al-7075 alloy [36–38]. An acceptable mechanism for the decline of boundary misorientations formed at elevated temperatures has been proposed by Yamashita et al. [39]. It was found that the formation of new grains during ECAP has been proposed as a result of the transformation of low angle boundaries (LABs) formed at early stages of deformation into HABs accompanied by dynamic recovery during hot deformation. The transition of LABs into HABs can be controlled by recovery rate which is accelerated with increasing temperature. At the higher pressing temperatures the rate of recovery increases and therefore annihilation of dislocations within the subgrains becomes easier, and consequently the absorption of dislocations into LABs becomes less frequent. This suggests that the evolution of the microstructure into an array of high angle boundaries is more difficult at the higher pressing temperatures.

Details on precipitation characteristics of 3 passes ECAPed specimens at RT before and after post-ECAP peak aging treatment (aging 9 h at 120 °C) are depicted in Fig. 9. As shown in Fig. 9(a) before aging no precipitate is visible in the TEM micrograph of ECAPed specimen at RT, but after aging

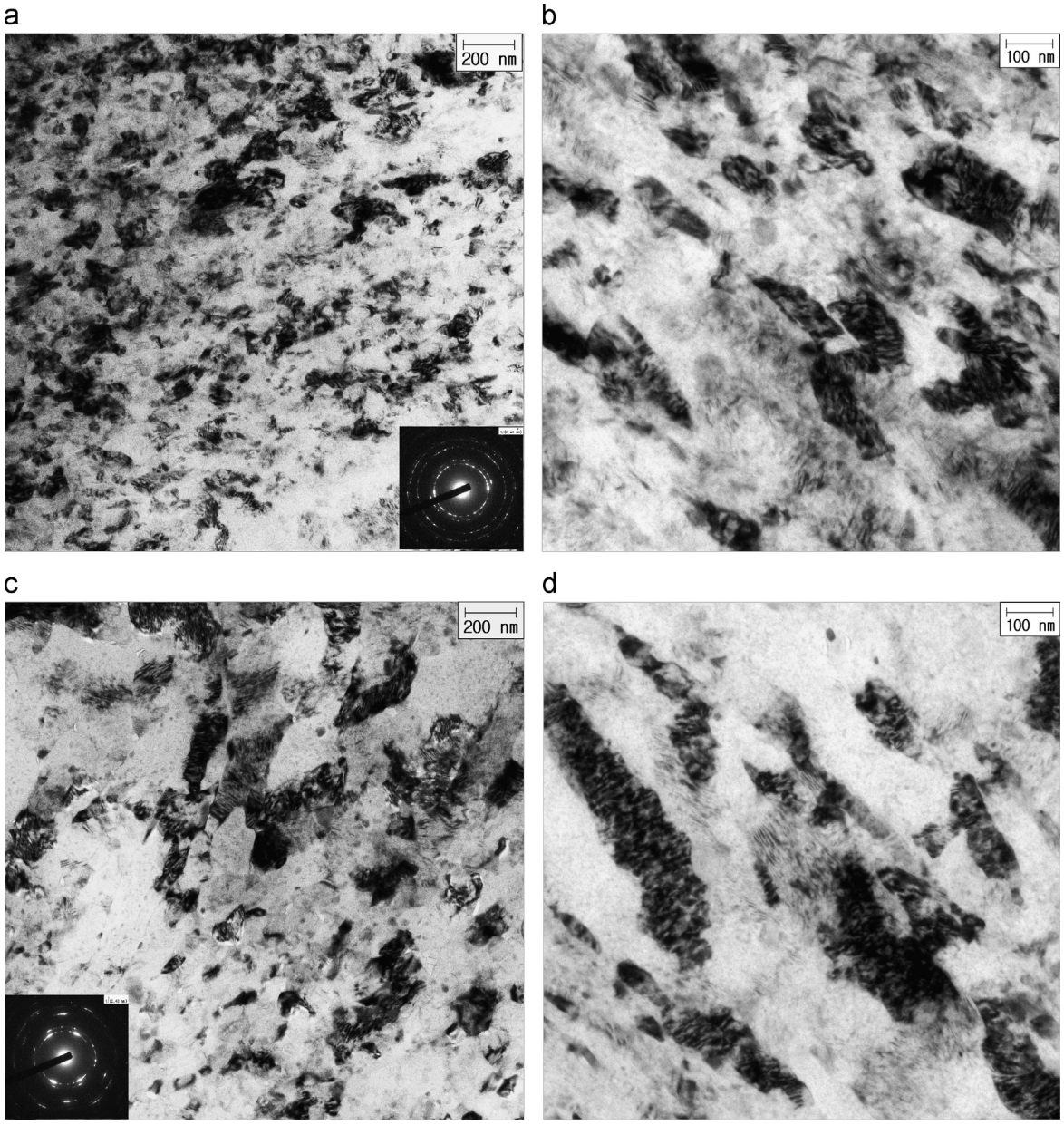

Fig. 7. TEM micrographs and corresponding SAED patterns of Al-7075 alloy subjected to three passes of ECAP process by route B_C at different temperatures, (a), (b) room temperature and (c),(d) 120 °C.

(Fig. 9(b) and (c)) small η′ precipitates with a size in range of 5–10 nm are present in the microstructure. The volume fraction of η′ phase in post ECAPed peak aged specimen is about 4.6%. XRD and TEM investigations demonstrate that G-P zones form during ECAP process at RT (as stated previously G-P zones are not visible in TEM images) and this G-P zones transform to metastable η′ phase during post-ECAP age hardening.

Effect of post-ECAP peak aging treatment (aging 6 h at 120 °C) on precipitates of 3 passes ECAP processed specimens at 120 °C is shown in Fig. 10. Careful inspection of precipitates in Fig. 10 and XRD data in Fig. 5 demonstrates that G-P zones and η′ phase coexist in the microstructure before aging, while the microstructure mainly consists of η′ phase after post-ECAP aging. So it can be concluded that most of the G-P zones transform to η′ phase during post-ECAP age hardening. Another important finding from Fig. 10 is that size of the η′ phase increases from about 3–5 nm to 5–10 nm after post-ECAP aging and also the volume fraction of η′ precipitates increases from 3.2% to 5.7% after post-ECAP aging.

As observed in this work, the different mechanical properties (strength and microhardness) of specimens in various ECAP and aging conditions are relevant to precipitates characteristics of specimens. TEM and XRD investigations indicate that, the reason of considerable increase in strength and microhardness during post-ECAP aging of ECAPed specimens at RT lies in transformation of G-P zones to η′ phase. On the other hand, during ECAP process of specimens at 120 °C considerable amount of η′ phase forms during ECAP, while no η′ phase forms during ECAP process of specimens at RT,

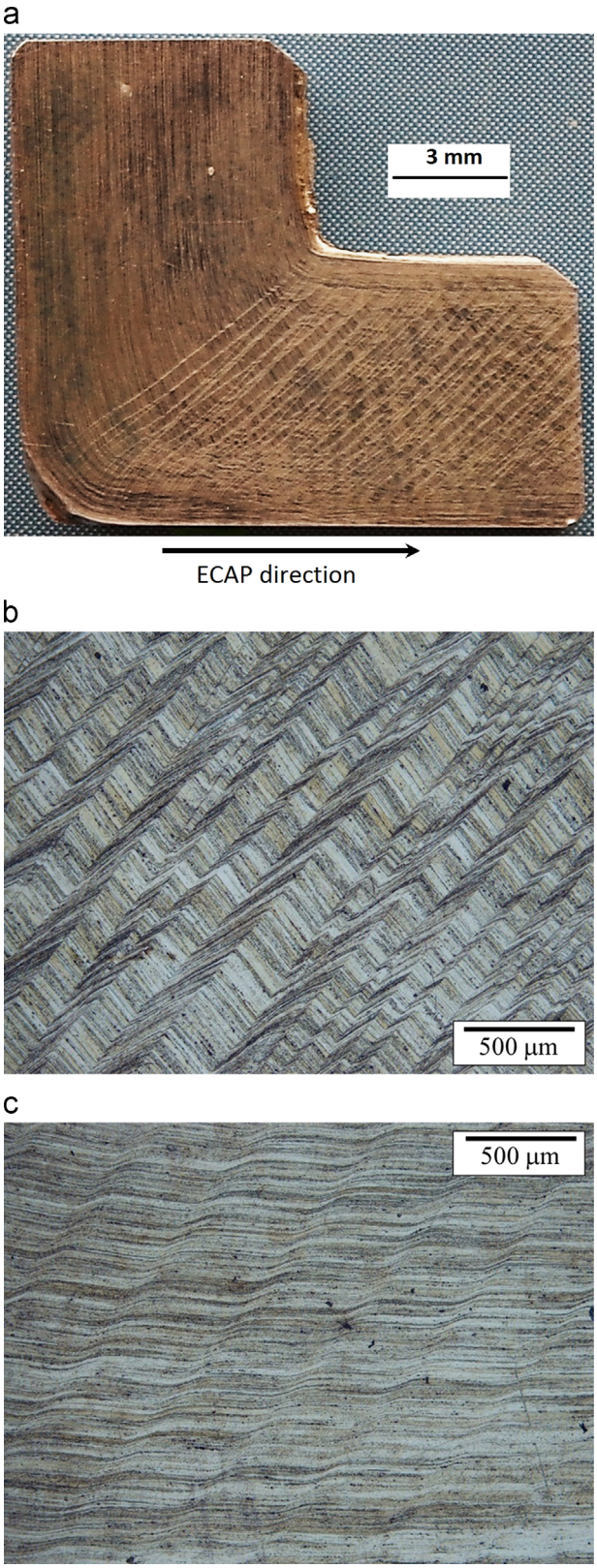

Fig. 8. Optical images of Al-7075 alloy after 1 pass of ECAP at different temperatures (longitudinal section), (a),(b) room temperature and (c) 120 °C.

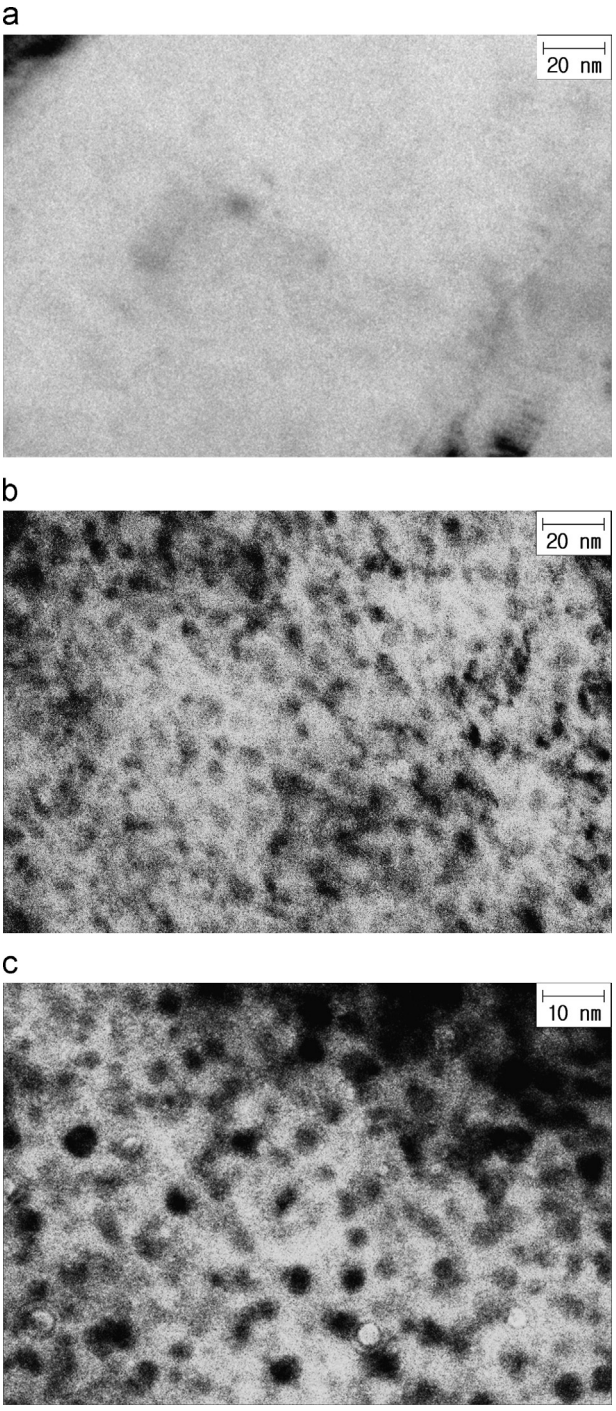

Fig. 9. TEM bright-field micrographs of three passes ECAPed Al-7075 alloy at RT, (a) before post-ECAP peak aging treatment and (b),(c) after post-ECAP peak aging treatment.

consequently the mechanical properties of ECAPed specimens at 120 °C are higher than those of ECAPed specimens at RT and also effect of post-ECAP aging on mechanical properties of ECAPed specimens at 120 °C is negligible. Finally, it can be concluded that the maximum hardness and strength could be reached during ECAP process of specimens at 120 °C by formation of G-P zones and η′ phase during dynamic strain aging and post-ECAP aging can be omitted. It should be noted that some G-P zones can be formed during the preheating time of the billet (before starting ECAP at 120 °C), however as the specimens have endured not an elongated preheating process

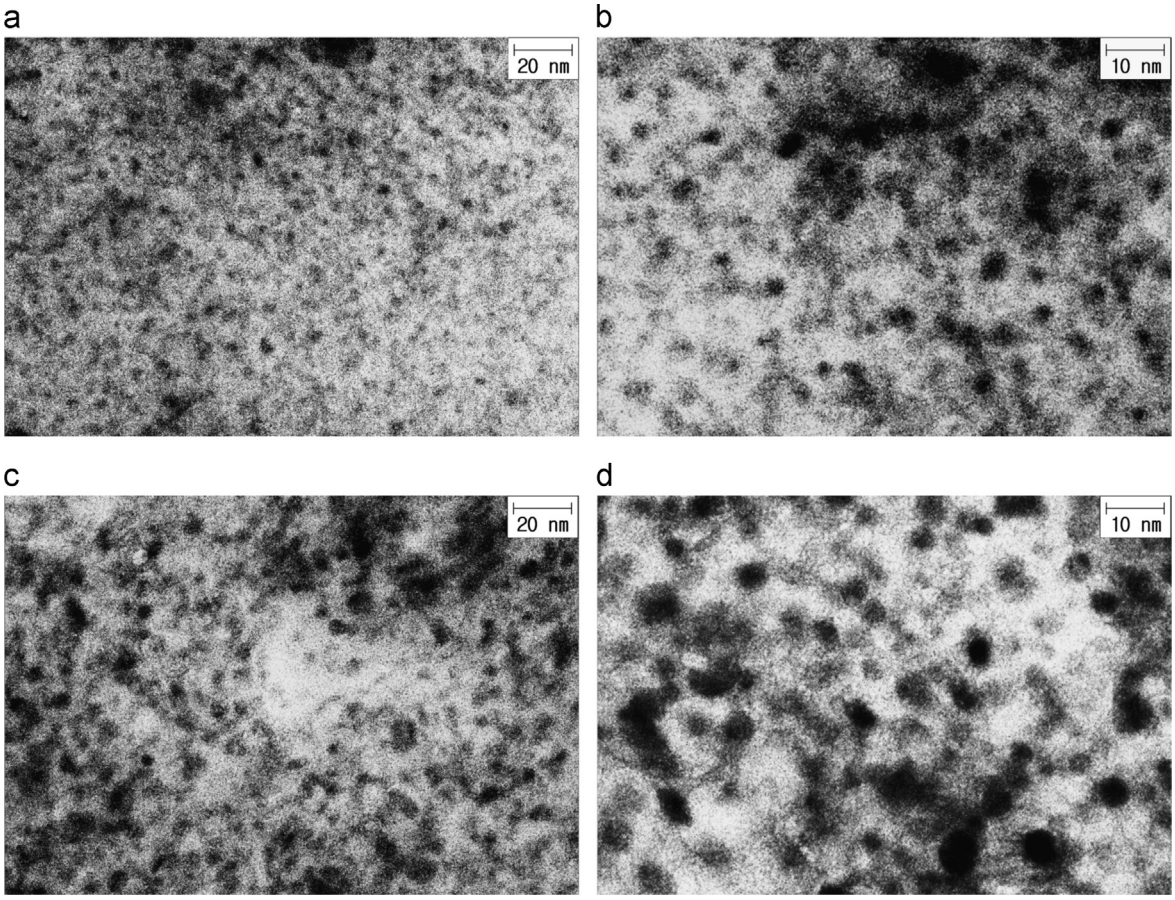

Fig. 10. TEM bright-field micrographs of three passes ECAPed Al-7075 alloy at 120 °C, (a),(b) before post-ECAP peak aging treatment, and (c),(d) after post-ECAP peak aging treatment.

(no more than 5 min), the ECAP at 120 °C was found to be more effective on formation of the G-P zones and η´ precipitates.

Based on the results obtained, it can be concluded that, ECAP process of Al-7075 alloy at RT and 120 °C in solid solution condition does not change the expected precipitation sequence for conventional aging treatment (G-P zones →η´ →η), but it accelerates the precipitation rate and decrease post-ECAP aging time for attaining maximum mechanical properties. The reason of accelerating the precipitation rate lies in the formation of suitable nucleation site and also increasing diffusion rate during ECAP. Suitable nucleation sites such as dislocations, deformation bands, shear bands, interfaces etc. increase significantly in ECAP process, so it can be concluded that ECAP process facilitates the precipitates nucleation. On the other hand, the diffusion of alloying elements which is required for precipitates formation, increases during ECAP as a result of increment in amount of dislocations, grain boundaries, interfaces and vacancies [27,40–43].

4. Conclusions

- The average microhardness and strength of ECAPed specimens at 120 °C are about 35% and 10% higher than those of unECAPed specimens in T6 condition and ECAPed specimens at room temperature, respectively. It is clear from these observations that effect of post-ECAP aging on mechanical properties of specimens ECAPed at 120 °C is negligible, while for ECAPed specimens at RT the mechanical properties increase about 5–10% during post-ECAP aging. The microhardness measurement reveals that ECAP process of solid solution Al-7075 alloy causes a significant decrease on post-ECAP aging time for attaining peak microhardness.
- Based on the microstructure observations by TEM and optical microscopy, the initial average grain size of about 60 μm was refined down to about 200–350 nm and 300–500 nm after three passes of ECAP process at room temperature and 120 °C, respectively. TEM investigations demonstrate that the grains after three passes of ECAP are reasonably equiaxed and high density of dislocations is present. SAED analysis reveals that most of the grain boundaries have high angles of misorientation.
- Precipitate characteristics by TEM and XRD indicate that the maximum mechanical properties may be mainly attributed to the presence of the fine dispersion of small η´ phase. ECAP process of Al-7075 alloy in solid solution condition accelerates the precipitation rate, and the precipitation rate is further accelerated by increasing ECAP temperature. Therefore it is feasible to form fine dispersion of small η´

precipitates during ECAP process at 120 °C and omit post-ECAP aging treatment.

References

[1] R.Z. Valiev, T.G. Langdon, Prog. Mater. Sci. 51 (2006) 881–981.
[2] C.M. Cepeda-Jiménez, J.M. García-Infanta, E.F. Rauch, J.J. Blandin, O.A. Ruano, F. Carreño, Metall. Mater. Trans. A 43 (2012) 4224–4236.
[3] K.H. Kim, Y.B. Chun, S.K. Hwang, Prog. Nat. Sci.: Mater. Int. 21 (2011) 277–285.
[4] C. Xu, T.G. Langdon, Scr. Mater. 48 (2003) 1–4.
[5] C. Xu, T.G. Langdon, J. Mater. Sci. 42 (2007) 1542–1550.
[6] Z. Horita, T. Fujinami, M. Nemoto, T.G. Langdon, Metall. Mater. Trans. A 31 (2000) 691–701.
[7] M. Ebrahimi, F. Djavanroodi, Prog. Nat. Sci.: Mater. Int. 24 (2014) 68–74.
[8] M.H. Shaeri, M.T. Salehi, S.H. Seyyedein, M.R. Abutalebi, J.K. Park, J. Mater. Des. 57 (2014) 250–257.
[9] F. Djavanroodi, B. Omranpour, M. Ebrahimi, M. Sedighi, Prog. Nat. Sci.: Mater. Int. 22 (2012) 452–460.
[10] J.M. Garcia-Infanta, A.P. Zhilyaev, A. Sharafutdinov, O.A. Ruano, F. Carreno, J. Alloy. Compd. 473 (2009) 163–166.
[11] R. Jayaganthan, H.G. Brokmeier, B. Schwebke, S.K. Panigrahi, J. Alloy. Compd. 496 (2010) 183–188.
[12] R. Islamgaliev, N. Yunusova, I. Sabirov, A. Sergueeva, R.Z. Valiev, Mater. Sci. Eng. A 319–321 (2001) 877–881.
[13] M. Vaseghi, A. KarimiTaheri, S.I. Hong, H.S. Kim, J. Mater. Des. 31 (2010) 4076–4082.
[14] D. Song, A.B. Ma, J.H. Jiang, P.H. Lin, L.Y. Zhang, Prog. Nat. Sci.: Mater. Int. 21 (2011) 307–313.
[15] L.J. Zhenga, C.Q. Chena, T.T. Zhoua, P.Y. Liua, M.G. Zeng, Mater. Character. 49 (2003) 455–461.
[16] W.J. Kim, J.K. Kim, H.K. Kim, J.W. Park, Y.H. Jeong, J. Alloy. Compd. 450 (2008) 222–228.
[17] M. Vaseghi, H.S. Kim, J. Mater. Des. 36 (2012) 735–740.
[18] F. Djavanroodi, M.H. Shaeri, S. Ahmadi, M. Sedighi, M.T. Salehi, S.H. Seyyedein, J. Strain Anal. Eng. Des. 48 (2013) 512–521.
[19] M.R. Roshan, S.A. JenabaliJahromi, R. Ebrahimi, J. Alloy. Compd.. 509 (2011) 7833–7839.
[20] M.H. Shaeri, M.T. Salehi, S.H. Seyyedein, M.R. Abutalebi, J.K. Park, J. Alloy. Compd. 576 (2013) 350–357.
[21] K. Oh-Ishi, Z. Horita, M. Furukawa, M. Nemoto, T.G. Langdon, Metall. Mater. Trans. A 29 (1998) 2011–2013.
[22] V.V. Stolyarov, Y.T. Zhu, I.V. Alexandrov, T.C. Lowe, R.Z. Valiev, Mater. Sci. Eng. A 299 (2001) 59–67.
[23] R.Z. Valiev, I.V. Alexandrov, Y.T. Zhu, T.C. Lowe, J. Mater. Res. 17 (2002) 5–8.
[24] N. Krasilnikov, W. Lojkowski, Z. Pakiela, R. Valiev, Mater. Sci. Eng. A 397 (2005) 330–337.
[25] B. Huarte, C.J. Luis, I. Puertas, J. Leon, R. Luri, J. Mater. Process. Tech. 162–163 (2005) 317–326.
[26] Y. Iwahashi, M. Furukawa, Z. Horita, M. Nemoto, T.G. Langdon, Metall. Mater. Trans. A 29 (1998) 2245–2252.
[27] K.R. Cardoso, D.N. Travessa, W.J. Botta, A.M. Jorge Jr., Mater. Sci. Eng. A 528 (2011) 5804–5811.
[28] A.S. Khan, C.S. Meredith, Int. J. Plast. 26 (2010) 189–203.
[29] K. Furuno, H. Akamatsu, K. Oh-ishi, M. Furukawa, Z. Horita, T.G. Langdon, Acta Mater. 52 (2004) 2497–2507.
[30] Y.H. Zhao, X.Z. Liao, Z. Jin, R.Z. Valiev, Y.T. Zhu, Acta Mater. 52 (2004) 4589–4599.
[31] J.K. Park, A.J. Ardell, Metall. Mater. Trans. A 14 (1983) 1957–1965.
[32] J.K. Park, A.J. Ardell, Scr. Metall. 22 (1988) 1115–1119.
[33] J. Gjonnes, Chr. J. Simensens, Acta Metall 18 (1970) 881–890.
[34] P. Málek, M. Cieslar, R.K. Islamgaliev, J. Alloy. Compd. 378 (2004) 237–241.
[35] C.M. Cepeda-Jimenez, J.M. Garcia-Infanta, O.A. Ruano, F. Carreno, J. Alloy. Compd. 509 (2011) 9589–9597.
[36] P.W.J. Mckenzie, R. Lapovok, Y. Estrin, Acta Mater. 55 (2007) 2985–2993.
[37] T.G. Langdon, M. Furukawa, M. Nemoto, Z. Horita, JOM 52 (2000) 30–33.
[38] K. Nakashima, Z. Horita, M. Nemoto, T.G. Langdon, Acta Mater. 46 (1998) 1589–1599.
[39] A. Yamashita, D. Yamaguchi, Z. Horita, T.G. Langdon, Mater. Sci. Eng. A 287 (2000) 100–106.
[40] J.K. Kim, H.G. Jeong, S.I. Hong, Y.S. Kim, W.J. Kim, Scr. Mater. 45 (2001) 901–907.
[41] S. Dadbakhsh, A. KarimiTaheri, C.W. Smith, Mater. Sci. Eng. A527 (2010) 4758–4766.
[42] A. Gholinia, P.B. Prangnell, M.V. Markushev, Acta Mater. 48 (2000) 1115–1130.
[43] S.V. Divinski, J. Ribbe, D. Baither, G. Schmitz, G. Reglitz, H. Rosner, K. Sato, Y. Estrin, G. Wilde, Acta Mater. 57 (2009) 5706–5717.